Dewetting Transitions on Superhydrophobic Surfaces: When Are Wenzel Drops Reversible?

ARTICLE *in* THE JOURNAL OF PHYSICAL CHEMISTRY C · AUGUST 2013

Impact Factor: 4.77 · DOI: 10.1021/jp4053083

2 AUTHORS:

Jonathan B Boreyko
Oak Ridge National Laboratory
24 PUBLICATIONS **572** CITATIONS
SEE PROFILE

Charles Patrick Collier
Oak Ridge National Laboratory
81 PUBLICATIONS **6,238** CITATIONS
SEE PROFILE

THE JOURNAL OF PHYSICAL CHEMISTRY C

Article

pubs.acs.org/JPCC

Dewetting Transitions on Superhydrophobic Surfaces: When Are Wenzel Drops Reversible?

Jonathan B. Boreyko and C. Patrick Collier*

Center for Nanophase Materials Sciences, Oak Ridge National Laboratory, Oak Ridge, Tennessee 37831-6493, United States

Supporting Information

ABSTRACT: On superhydrophobic surfaces, drops in the Wenzel state can be switched to the suspended Cassie state in some cases but in other cases are irreversibly impaled in the surface roughness. To date, the question of when dewetting transitions are possible for Wenzel drops has not been resolved. Here, we show that pinned Wenzel drops being stretched out-of-plane cannot reduce their contact angle below a critical value where unstable pinch-off occurs, preventing dewetting for Wenzel drops that exhibit receding contact angles beneath this critical pinch-off angle. Dewetting transitions are therefore only possible for Wenzel drops with moderately large receding contact angles ($\theta_r \approx 90°$), which requires low surface roughness for one-tier surfaces or a Partial Wenzel wetting state for two-tier surfaces.

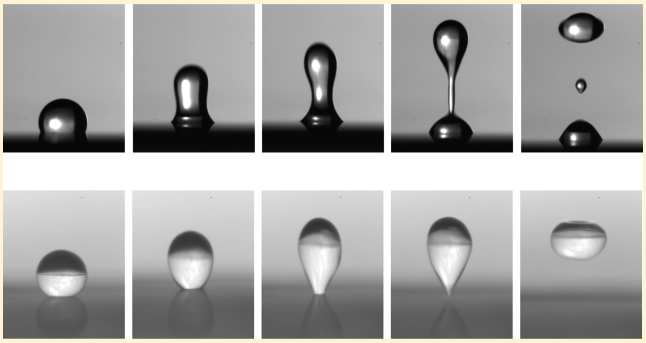

INTRODUCTION

Superhydrophobic surfaces are typically designed to suspend water in the mobile Cassie state; however, it is well-known that wetting transitions to an impaled Wenzel state frequently occur even when the Cassie state is energetically favorable.[1] Conditions known to trigger wetting transitions include mechanical compression,[2,3] underwater submersion beyond a critical hydrostatic pressure,[4,5] electrowetting,[6] evaporation to a higher Laplace pressure,[7,8] drop impact,[9,10] mechanical vibration,[11] or deceleration during drop deposition.[12] Perhaps even more problematic are condensate drops that nucleate from within the surface roughness, which typically form in a fully impaled Wenzel state on microscale-only roughness[3,13,14] and in a partially wetting state on nanoscale or hierarchical roughness.[15−18] Utilizing superhydrophobic surfaces with robust hierarchical roughness can maximize the energetic favorability of the Cassie state and delay the occurrence of wetting transitions,[19−23] but it is becoming increasingly clear that Wenzel states are still common in many systems.

Despite the endemic problem of superhydrophobic surfaces exhibiting Wenzel drops due to wetting transitions or condensation, the possibility of dewetting back to the suspended Cassie state has been largely ignored. This disregard of dewetting transitions was not borne out of neglect; rather, several reports convincingly demonstrated that the Cassie to Wenzel wetting transition was irreversible even when the Wenzel drop was mechanically forced[3,11] or when an electrowetting voltage was released.[6,24,25] A Wenzel to Cassie transition was accomplished by vaporizing a drop's liquid−solid interface via high-temperature heating,[26,27] but this method is impractical for many systems and does not preserve the drop's volume. A resurgent interest in dewetting was stoked by a recent report that deposited drops and condensate trapped in a Wenzel state on a lotus leaf could fully transition to the stable Cassie state when subjected to mechanical vibration.[16] A follow-up report using microfabricated surfaces found that hierarchical roughness is crucial for enabling dewetting transitions: Wenzel drops fully impaled in one-tier or two-tier roughness were indeed irreversible, but partial Wenzel drops wetting only one of two tiers could be effectively dewetted to the Cassie state.[28] Similar results were observed for hierarchical superhydrophobic surfaces submerged in water baths, where the partial Wenzel state could be dewetted to the Cassie state via negative pressure[29] or electrolysis.[30,31]

The irreversibility of Wenzel drops on certain superhydrophobic surfaces has previously been attributed to the energetic favorability of the Wenzel state,[3,11,29] but recently, dewetting transitions have been obtained even when the Cassie state is metastable.[27,32] Another common hypothesis is that an energy barrier prevents dewetting,[19,29,33] but this cannot explain why a Wenzel drop fails to dewet even when subjected to a strong out-of-plane force.[28] It is also unclear when dewetting is restricted to the Partial Wenzel state exclusive to hierarchical surfaces,[28,29,31] as several recent reports were able to obtain a Wenzel to Cassie transition for drops impaled in one-tier surfaces.[27,32,34] Therefore, it remains poorly understood when a dewetting transition from a Wenzel to Cassie state is possible.

Received: May 29, 2013
Revised: August 12, 2013
Published: August 12, 2013

   dx.doi.org/10.1021/jp4053083 | J. Phys. Chem. C 2013, 117, 18084−18090

Here, we use experiments and computer simulations to demonstrate that a pinned Wenzel drop experiencing an out-of-plane force cannot decrease its contact angle below a critical value where unstable pinch-off occurs. We show that a dewetting transition is only possible when the receding contact angle of a Wenzel drop is larger than this critical angle, such that the energy barrier for dewetting is lower than that for pinch-off. This is why dewetting transitions are only observed for Wenzel states exhibiting relatively large receding contact angles, such as partial Wenzel drops on two-tier superhydrophobic surfaces.

EXPERIMENTAL AND SIMULATION METHODS

Experimental Setup. A two-tier superhydrophobic surface composed of carbon nanotubes deposited onto silicon micropillars, along with equivalent one-tier surfaces exhibiting either micropillars or nanotubes, was fabricated in the same manner as a previous report.[20] On the two-tier surface, the carbon nanotubes were in-between and on top of the micropillars but did not cover the side-walls. A *Nelumbo Nucifera* lotus leaf, plucked fresh from the stem to within one day, was also used as a natural two-tier superhydrophobic surface for select experiments.

The Cassie state is thermodynamically more stable than the Wenzel state when the Young's contact angle exceeds a critical value:[3,35,36]

$$\theta_Y > \theta_c,\ \cos(\theta_c) = -\frac{1-f}{r-f} \tag{1}$$

where f is the solid fraction and r is the surface roughness ratio. For the synthetic surfaces used here, a coating of 1-hexadecanethiol exhibited θ_Y = 101°, while the surface parameters of the micro-only, nano-only, and two-tier surfaces yield θ_c =122°, 96°, and 94°, respectively.[20] It is more complex to estimate the surface energy and geometry of a lotus leaf; however, they are generally considered to exhibit a thermodynamically stable Cassie state.[37] Therefore, the Cassie state is energetically favorable for all of these surfaces (eq 1), with the exception of the micro-only surface where the Cassie state is metastable.[20,28]

Metastable Wenzel drops were trapped in the surface roughness in two different ways: by depositing drops with a partial concentration of ethanol and waiting for the ethanol to preferentially evaporate or by growing condensation on the surface using a circulating chiller.[16] To distinguish between the two different Wenzel states possible on the two-tier surfaces, the term "partial Wenzel" refers to drops impaling the microroughness but not the nanoroughness, while "full Wenzel" refers to drops impaling both tiers.[28] When using the deposition method on the one-tier surfaces, the initial drop volume was 2.0 μL, and the initial ethanol concentration (by volume) was 12.5% on the micropillars and 17.5% on the nanotubes. On the two-tier surface, the deposited drop volume was 2.25 μL, and the concentration of ethanol was 25−27.5% for partial Wenzel drops and 32.5% for full Wenzel drops. Obtaining and characterizing various wetting states on a two-tier surface using a wide range of ethanol concentrations was more fully detailed in a previous report.[28] On the disordered lotus leaf, the distinction between partial Wenzel and full Wenzel wetting states was less discrete, but drops with 33% or 50% ethanol were used to obtain Wenzel drops with varying degrees of hysteresis.

A dewetting transition was attempted by vertically vibrating the Wenzel drops using a speaker cone (KLH Audio B-Pro6) connected to a sinusoidal signal generator (Agilent 33220A 20 MHz). For drops with an initial concentration of ethanol, the drop was not vibrated until its evaporation rate followed the d^2 law, which usually required about 5 min for the drops used here. This d^2 law, which states that the square of a drop's diameter decreases linearly with time for a single-component drop, signifies that the drop is now almost entirely composed of water (which evaporates about 5 times slower than ethanol).[16,28] A frequency of 100 Hz was used to promote vibration near the drop's second resonance mode,[16,38] and the amplitude was gradually increased until the Wenzel drop either experienced a dewetting transition or pinch-off. Side-view high-speed imaging of the drop dynamics was obtained with a Phantom v7.1 camera attached to an Infinity K2 microscope.

Surface Evolver Simulations. The Surface Evolver program[39] was used to characterize the shape and stability of pinned Wenzel drops being stretched out-of-plane from the surface. Surface Evolver obtains the equilibrium shape of liquids using a finite element method, where a triangular mesh of vertices is iteratively evolved until the system's free energy is minimized. Previous reports have utilized Surface Evolver to model the deformation of compressed[40] or tilted[41] drops on superhydrophobic surfaces, with excellent agreement to the experimental results.

Here, the liquid−air interface of a pinned drop was represented by 15,457 vertices, 46,176 edges, and 30,720 facets in three-dimensional space. This fine mesh allowed for contact angle measurements that were accurate to within 1°. No facets were used to simulate the liquid−solid contact area since for Wenzel drops this area is typically fixed and not governed by surface energy minimization. Instead, the Wenzel drop's pinned contact line was enforced by imposing a fixed circular boundary for all vertices and edges located on the surface (z = 0). This approach of not directly simulating the contact area has the added benefit of being applicable for any pinned drop regardless of its underlying surface roughness or specific wetting state. The solid substrate was effectively introduced by constraining all vertices to be nonnegative in value for their z-coordinates. The drop's physical parameters were held constant at V = 10 μL, ρ = 998 kg/m^3, and γ = 0.0728 N/m, while the density of the surrounding air was neglected. The initial contact angle of a simulated Wenzel drop at zero gravity, θ_i, was varied in 15° increments. For each value of θ_i, the imposed radius of the pinned contact line was determined for a spherical-cap drop from the geometrical relationship

$$a = \sin\theta_i\left(\frac{3V}{\pi(1-\cos\theta_i)^2(2+\cos\theta_i)}\right)^{1/3} \tag{2}$$

For a pinned drop with a given initial contact angle, θ_i, the out-of-plane acceleration was increased in increments of 5 or 10 m/s^2 until reaching the final possible equilibrium state, which was found to the nearest integer value of g. For each value of g, the equilibrium state was found by minimizing the free energy of the system given by

$$E = E_S - U = \gamma A_{LG} - g\rho \iiint z\,dx\,dy\,dz \tag{3}$$

where E_S corresponds to the surface energy of the drop's interface, U denotes the potential energy provided by the out-of-plane acceleration, and A_{LG} is the total surface area of the

dx.doi.org/10.1021/jp4053083 | J. Phys. Chem. C 2013, 117, 18084−18090

liquid−air interface. To obtain equilibrium, E was iterated until converging to 10^{-5} significant digits (for example, E = 1.40816 μJ). An equilibrium shape could not be obtained for values of g above the critical threshold, where it became energetically favorable for the neck of a stretched drop to collapse to the pinch-off singularity. Previous works have modeled droplets falling from a flowing capillary tube by using Navier−Stokes equations to examine the necking dynamics close to the pinch-off singularity.[42−44] Here, we focus instead on the static equilibrium shapes of constant-volume drops stretched by various gravitational energies in order to determine which range of contact angles a pinned drop may stably exhibit before destabilizing toward the pinch-off singularity.

RESULTS AND DISCUSSION

Experimental Results. Wenzel drops were unable to experience a dewetting transition during vibration on the one-tier superhydrophobic micropillars (Figure 1a) or nanotubes

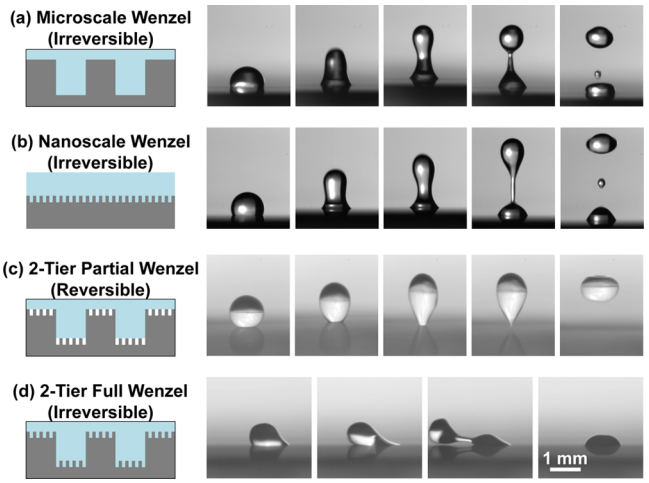

Figure 1. Wenzel drops were mechanically vibrated at 100 Hz until they experienced either unstable pinch-off or a dewetting transition to the Cassie state. (a,b) Wenzel drops on one-tier superhydrophobic surfaces were irreversibly impaled in the surface roughness, but (c) partial Wenzel drops wetting only one of two tiers on a hierarchical surface exhibited dewetting to the stable Cassie state. (d) The extremely low receding contact angle of full Wenzel drops was demonstrated by using a nitrogen gun to maximally deform the drop, whose contact line could not recede even as $\theta \rightarrow 0°$. The peak-to-peak vibrational amplitudes were measured by a high-speed camera to be (a) 0.73, (b) 0.54, and (c) 0.30 mm. Movies M1−M4 are available in the Supporting Information.

(Figure 1b). As the vibrational amplitude was continuously increased, the Wenzel drops eventually experienced pinch-off, but the lower portion of the drop remained fully impaled in the surface roughness with an unchanged contact diameter. On the two-tier surfaces, the ability for a Wenzel drop to dewet is dependent on whether it is impaling both tiers of roughness or only one of the two tiers.[28,29] A partial Wenzel drop wetting only the microscale but not the nanoscale was able to undergo a dewetting transition to the stable Cassie state with minimal vibrational amplitude (Figure 1c), but full Wenzel drops impaling both tiers of roughness were irreversible in the same manner as Wenzel drops on the one-tier surfaces (Figure 1d).

The inability of a Wenzel drop to dewet is particularly notable on the one-tier nanotubes and two-tiered surfaces where the Cassie state is energetically favorable,[28] as evidenced by the sheared portion of the drop bouncing in the Cassie state upon rebound (see Movie S2 in the Supporting Information). Therefore, the irreversibility of the Wenzel state cannot be attributed to either the presence of a dewetting energy barrier (which would eventually be overcome by the increasing vibrational amplitude) or to the energetic favorability of the Wenzel state (the Cassie state is stable). Rather, it would appear that the energy barrier for unstable pinch-off is lower than the energy barrier for dewetting, preventing a dewetting transition from occurring even when the drop is mechanically forced.

This competition between dewetting and pinch-off can be elucidated by recalling that the dewetting transition for drops is driven by the contact line.[16,28] For a Wenzel drop to achieve a dewetting transition, its contact diameter must recede to zero from *all* sides. Once the contact line has finished unzipping, the drop is completely freed from the surface roughness and switches to the suspended Cassie state. Note that a dewetting transition is fundamentally different from overcoming contact angle hysteresis, which merely translates the drop across the surface in its existing wetting state. Since the contact line of a Wenzel drop is initially pinned, the drop must be stretched out-of-plane from the surface until its apparent contact angle uniformly reduces to its receding value to enable the dewetting transition. It can be seen in Figure 1c that the receding contact angle of partial Wenzel drops is relatively large (θ_r >90°), while Figure 1d conveys the extremely low receding contact angle of full Wenzel drops ($\theta_r \rightarrow 0°$). It is hypothesized here that the large receding contact angle of partial Wenzel drops enables dewetting to occur at minimal drop deformation, while the very low receding contact angle of full Wenzel drops promotes shape-induced pinch-off to occur before the drop could deform enough to attain θ_r. This hypothesis will now be examined using Surface Evolver simulations.

Surface Evolver Results. The Surface Evolver program was used to stretch pinned drops to various equilibrium shapes by applying an out-of-plane acceleration. The potential energy acting to stretch the drop can be nondimensionalized:

$$U^* = \frac{U}{\gamma V^{2/3}} \tag{4}$$

such that the stretched drop shape for a given θ_i and U^* is the same for any value of V, γ, or ρ. With increasing U^*, the drop's apparent contact angle decreases until reaching a critical minimal value, θ_c, beyond which shape-induced pinch-off occurs (Figure 2). It can be seen that the critical values of U_c^* and θ_c depend on the pinned drop's initial contact angle, θ_i, which governs the shape of drop deformation during stretching.

The dependence of U_c^* and θ_c on θ_i can perhaps best be characterized by measuring the evolving radii of curvature of a drop at each equilibrium value of U^* (Figure 3). Here, two different radii of curvature were measured for each equilibrium state: the curvature at the contact line (R_1) and the curvature at the top of the drop (R_2). The values of R_1 and R_2 were found by recording the coordinates of three adjacent vertices at each region of interest and extrapolating the equation for a circle. At U^* = 0, the drop has a spherical-cap shape (top series in Figure 2), and therefore, $R_1 = R_2$. As U^* increases, the curvature of R_1 approaches infinity (middle series in Figure 2) and then assumes a negative value (bottom series in Figure 2). It can be seen in Figure 3 that regardless of the drop's initial contact angle, θ_i, the drop becomes unstable as the negative curvature

dx.doi.org/10.1021/jp4053083 | J. Phys. Chem. C 2013, 117, 18084−18090

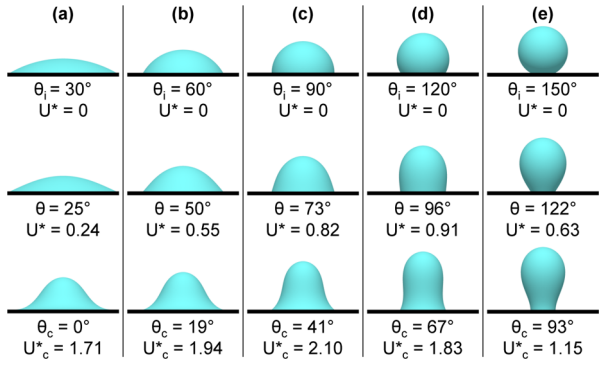

Figure 2. Simulation of pinned drops at equilibrium for a given initial contact angle of (a) 30°, (b) 60°, (c) 90°, (d) 120°, and (e) 150°. As each drop becomes stretched by a dimensionless potential energy, U^*, its equilibrium contact angle shrinks until reaching a critical minimal value, θ_c, beyond which the drop becomes unstable due to shape-induced pinch-off.

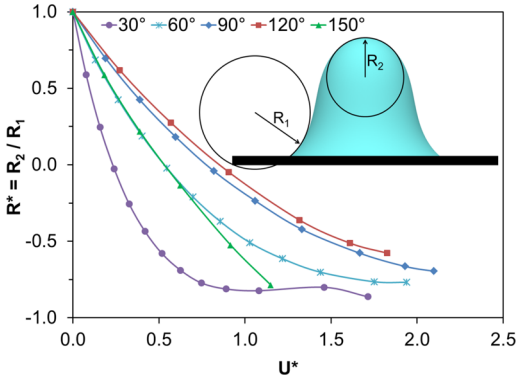

Figure 3. Drops cannot be stretched beyond a critical curvature of $R_c^* \approx -1$, where pinch-off becomes energetically favorable due to the negative curvature at the neck of the drop. The legend refers to a pinned drop's initial contact angle (θ_i), and the final data point for each drop corresponds to the critical dimensionless potential energy (U_c^*) beyond which an equilibrium state is not possible.

at the bottom of the drop approaches the magnitude of the positive curvature at the top of the drop:

$$R_c^* = \frac{R_2}{R_1} \approx -1 \tag{5}$$

The Surface Evolver simulations suggest that it is impossible for a pinned Wenzel drop to decrease its contact angle beneath a critical value θ_c. When plotting the simulated value of θ_c as a function of the initial contact angle θ_i (Figure 4), a linear relationship is revealed:

$$\theta_c = a\theta_i + b \tag{6}$$

where $a = 0.79 \pm 0.05$ and $b = -28° \pm 5°$ to within a 95% confidence interval. This reveals that only pinned drops with hydrophilic contact angles ($\theta_i < 35°$) can exhibit a stable contact angle of $\theta \to 0°$ when forced out-of-plane from the surface. In all other cases, drops cannot exhibit contact angles beneath a nonzero value of θ_c due to pinch-off occurring.

Phase Diagram and Discussion. The practical implication of eq 6 is that Wenzel drops can only dewet when their receding contact angle is larger than this critical value:

$$\theta_r > 0.79\theta_i - 28° \tag{7}$$

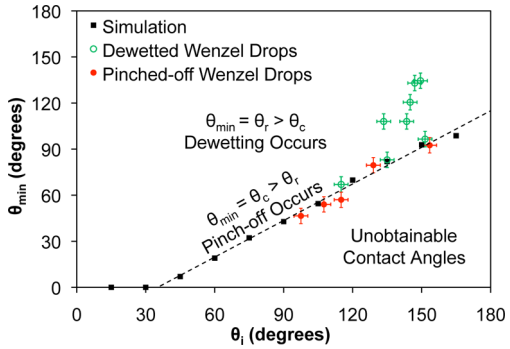

Figure 4. Phase diagram depicting when a dewetting transition is possible for Wenzel drops on superhydrophobic surfaces. The minimum contact angle (θ_{min}) a stretched drop can exhibit will either be the dewetting angle (θ_r) or the critical pinch-off angle (θ_c) depending on which is larger. For drops where pinch-off occurs, the experimental value of θ_c is in agreement with the simulated value denoted by the dashed line (eq 6). Experimental data includes Wenzel drops on one-tier surfaces and partial and full Wenzel drops on two-tier surfaces. See Table 1 for more information.

such that the contact line is able to uniformly recede before pinch-off can occur. This agrees very well with the experimental data, where partial Wenzel drops were observed to dewet with a receding contact angle $\theta_r > \theta_c$, while Wenzel and full Wenzel drops exhibited unstable pinch-off at contact angles in agreement with the simulated value of θ_c (Figure 4). For the Wenzel drops experiencing pinch-off, the experimental value of θ_c was measured as a stretched drop's lowest obtainable contact angle, which was observed to remain constant to within ±5° during pinch-off (error bars in Figure 4).

An intriguing implication of eq 7 is that an initially irreversible Wenzel drop may later become reversible if it loses some of its volume to change its contact angle. For example, suppose a Wenzel drop exhibited an initial contact angle of $\theta_i = 135°$ and a receding contact angle of $\theta_r = 50°$. Initially, $\theta_c = 79°$ (eq 7), such that unstable pinch-off would occur during a first attempt at dewetting ($\theta_c > \theta_r$). However, this pinch-off would reduce the volume of the pinned drop and therefore also reduce its apparent contact angle. If this new contact angle were $\theta_i = 90°$, for example, now $\theta_c = 43°$, which should enable dewetting ($\theta_r > \theta_c$). Unfortunately, this could not be tested here, as the values of θ_r were either prohibitively low (for Wenzel and full Wenzel drops) or too high (partial Wenzel). In the future, a one-tier surface with low surface roughness and moderate θ_r could be employed to test this predictive hypothesis. Indeed, an extremely recent report was published after the submission of this article that already supports the hypothesis of shape-dependence. Drops were deposited onto one-tier honeycomb structures and stretched out-of-plane using a superhydrophilic cap that was fixed to the opposing side of the drop.[45] This superhydrophilic cap exhibited a fixed diameter, such that the contact angle a drop makes with the cap would increase with drop volume. Sure enough, drops exhibiting larger volumes (8 μL) could not be dewetted from the honeycomb structures due to pinch-off occurring, while smaller drops (4 μL) could completely dewet without any pinch-off.[45] This applied not only to the honeycomb structures but also to a smooth surface, indicating that eq 7 is useful for both smooth and structured surfaces. While this system is not perfectly analogous due to the drop being pinned between two different surfaces instead of

dx.doi.org/10.1021/jp4053083 | J. Phys. Chem. C 2013, 117, 18084−18090

Table 1. Summary of Experimental Results Depicted in Figure 4, where θ_i Is the Initial Contact Angle of a Partial Wenzel (PW) or Wenzel Drop, θ_{min} Is the Minimum Possible Contact Angle Obtained during Vibration, and θ_c Is the Critical Angle Where Pinch-off Is Predicted to Occur (eq 7); in Every Case Where Dewetting Was Successful, $\theta_{min} = \theta_r > \theta_c$; in Every Case Where Pinch-off Occurred Instead of Dewetting, $\theta_{min} \approx \theta_c > \theta_r$

initial wetting state	surface	θ_i	θ_{min}	θ_c	method	result
PW (deposited)	2-tier chip	144°	108°	86°	vibration	dewet
PW (deposited)	2-tier chip	134°	108°	78°	vibration	dewet
PW (deposited)	lotus leaf	152°	97°	92°	vibration	dewet
PW (deposited)	lotus leaf	145°	121°	87°	vibration	dewet
PW (condensed)	lotus leaf	150°	135°	91°	vibration	dewet
PW (condensed)	lotus leaf	147°	133°	89°	vibration	dewet
Wenzel (deposited)	micropillars	115°	67°	63°	heating[27]	dewet
Wenzel (deposited)	micropillars	135°	83°	79°	magnet[32]	dewet
Wenzel (deposited)	lotus leaf	154°	93°	94°	vibration	pinch-off
Wenzel (deposited)	lotus leaf	129°	80°	74°	vibration	pinch-off
Wenzel (deposited)	lotus leaf	108°	54°	57°	vibration	pinch-off
Wenzel (deposited)	nanotubes	115°	57°	63°	vibration	pinch-off
Wenzel (deposited)	micropillars	98°	47°	49°	vibration	pinch-off

exhibiting a free surface, it still indicates that the ability to dewet depends on the contact angle(s) of the pinned drop. In short, for a drop exhibiting a fixed contact diameter, decreasing its volume serves to decrease its contact angle, which increases the possibility of dewetting by delaying the onset of pinch-off (eq 7). In many cases, however, it is still desirable for a drop to experience a dewetting transition without any loss of volume. For this reason, a Wenzel drop is referred to here as irreversible if it cannot experience a dewetting transition while preserving its initial volume.

While the Surface Evolver simulations obtain a pinned drop's equilibrium shape for a constant out-of-plane acceleration, the experimentally vibrated drops are not at equilibrium due to a constantly fluctuating acceleration. For this discrepancy to be reasonably small, the surface tension of a vibrated drop should be dominant over its inertial effects, so that the drop can approximate its equilibrium shape at each stage of acceleration. The maximum velocity experienced by a vibrating drop is given by $V = 2\pi fA$, where f is the frequency and A is half of the peak-to-peak amplitude. A drop's Weber number, which compares the energy of inertia to the energy of surface tension, may be estimated by

$$We = \frac{\rho(2\pi fA)^2 R}{\gamma} \tag{8}$$

where R is the initial radius of the drop. For the vibrated drops in Figure 1a–c, We = 0.39, 0.23, and 0.07, respectively, indicating that surface tension indeed dominates over inertial effects ($We < 1$).

On the basis of Figure 4, it is likely that the reversibility of a Wenzel drop is not explicitly dependent on its specific wetting state, but rather on its contact angle hysteresis. While it is still difficult to theoretically model the contact angle hysteresis of drops on roughened surfaces, it is becoming increasingly clear that the hysteresis is governed by the localized pinning of the receding contact line on surface features.[46−49] The extent of contact line pinning is dependent on the degree of surface roughness and on the wetting state of the liquid.[50] The surface roughness of a two-tier surface is typically an order of magnitude larger than a one-tier surface,[20] which is why full Wenzel drops exhibit an extremely large contact angle hysteresis and are irreversibly impaled. Partial Wenzel drops on two-tier surfaces are easily dewetted because the partial presence of air pockets significantly lowers the contact angle hysteresis compared to full Wenzel drops (Figure 1c,d). While Full Wenzel drops are generally irreversible and partial Wenzel drops are generally reversible, the dewetting of Wenzel drops on one-tier surfaces must be taken on a case-by-base basis. Many one-tier surfaces cannot achieve dewetting transitions for Wenzel drops (Figure 1a,b), but others are capable of dewetting when the contact angle hysteresis is small enough to satisfy eq 7. For example, a previously reported micropillared surface exhibited a relatively large receding contact angle of $\theta_r \approx 83°$ for Wenzel drops and was able to dewet to the Cassie state (Table 1).[32] However, the problem with low-roughness one-tier surfaces is that the Wenzel state is typically the energetically favorable configuration, such that the dewetted Cassie state is metastable and fragile. Robust superhydrophobic surfaces require large aspect-ratio roughness features, in which case only partial Wenzel drops on hierarchical surfaces seem viable for dewetting. Since smooth surfaces also exhibit contact angle hysteresis, the competition between dewetting and pinch-off captured by eq 7 should be applicable to drops on smooth surfaces as well as structured surfaces. The fundamental difference is that drops dewetting from smooth surfaces cannot exhibit a dewetting transition to a new wetting state; if allowed to return to the substrate, drops will resume their initial contact angle.

Thus far, only contact-line driven dewetting has been observed for Wenzel drops.[16,28,32] Without resorting to the vaporization of the interface,[26,27] it remains unknown whether partial Wenzel drops could also dewet via the out-of-plane receding of the microscopic liquid–vapor menisci distributed throughout the drop's contact area, as has been observed in the absence of a contact line for two-tier superhydrophobic surfaces submerged in a water bath.[29]

A brief discussion is warranted for the specific case of condensation. Using an environmental scanning electron microscope, it has recently been observed that superhydrophobic condensate typically nucleates *within* a unit cell(s) of surface roughness, but proceeds to grow outward in a suspended Cassie state on sufficiently robust nanoroughness.[17,18,36,51] The base of such a balloon-shaped condensate drop is impaled in the middle but suspended on the outside, known as a partially wetting state.[17] While such drops have been observed to successfully dewet from the surface via

dx.doi.org/10.1021/jp4053083 | J. Phys. Chem. C 2013, 117, 18084−18090

vibration[16] or coalescence-induced jumping,[52−54] it is possible that a nanoscale footprint remains impaled in the original unit cell(s) if $\theta_c > \theta_r$ in this localized area. This could potentially explain the recent observation that, after a condensate drop departs the surface, the site promotes the preferential growth of future drops, suggesting that the area could remain partially wetted.[51]

CONCLUSIONS

In conclusion, a dewetting transition from a Wenzel state to the Cassie state is only possible when the Wenzel drop's receding contact angle is larger than a critical angle where unstable pinch-off occurs. Using experiments in conjunction with computer simulations, we have shown that this critical angle can be predicted from the apparent contact angle of a Wenzel drop. Wenzel drops can be dewetted on one-tier surfaces exhibiting only a moderate surface roughness and hysteresis, but the resulting Cassie state is typically metastable and fragile. The increased roughness of a hierarchical superhydrophobic surface serves to stabilize the Cassie state, but full Wenzel drops impaled in both tiers will pinch-off before dewetting occurs due to their extremely low receding contact angle. Drops in a partial Wenzel state on a hierarchical superhydrophobic surface, however, are both easily dewetted and also exhibit a stable and robust Cassie state. This improved understanding of dewetting transitions is expected to better facilitate reversible switching between high-adhesion and low-adhesion wetting states on superhydrophobic surfaces. Since our model is solely a function of contact angle and contact angle hysteresis, it will also be useful for the controlled dewetting (or pinch-off) of drops from smooth surfaces.

ASSOCIATED CONTENT

Supporting Information

Four videos corresponding to Figure 1. This material is available free of charge via the Internet at http://pubs.acs.org.

AUTHOR INFORMATION

Corresponding Author

*(C.P.C.) E-mail: colliercp@ornl.gov. Phone: (865) 576-3638.

Notes

The authors declare no competing financial interest.

ACKNOWLEDGMENTS

The experimental data for Figures 1 and 4 were obtained at Duke University in the Department of Mechanical Engineering and Materials Science. The authors thank Chuan-Hua Chen for the use of his lab. This research was conducted at the Center for Nanophase Materials Sciences, which is sponsored at Oak Ridge National Laboratory by the Scientific User Facilities Division, Office of Basic Energy Sciences, U.S. Department of Energy.

REFERENCES

(1) Quere, D. Wetting and Roughness. *Annu. Rev. Mater. Res.* **2008**, *38*, 71−99.
(2) Bico, J.; Marzolin, C.; Quere, D. Pearl Drops. *Europhys. Lett.* **1999**, *47*, 220−226.
(3) Lafuma, A.; Quere, D. Superhydrophobic States. *Nat. Mater.* **2003**, *2*, 457−460.
(4) Herminghaus, S. Roughness-Induced Non-Wetting. *Europhys. Lett.* **2000**, *52*, 165−170.
(5) Bobji, M. S.; Kumar, S. V.; Asthana, A.; Govardhan, R. N. Underwater Sustainability of the "Cassie" State of Wetting. *Langmuir* **2009**, *25*, 12120−12126.
(6) Krupenkin, T. N.; Taylor, J. A.; Schneider, T. M.; Yang, S. From Rolling Ball to Complete Wetting: The Dynamic Tuning of Liquids on Nanostructured Surfaces. *Langmuir* **2004**, *20*, 3824−3827.
(7) McHale, G.; Aqil, S.; Shirtcliffe, N. J.; Newton, M. I.; Erbil, H. Y. Analysis of Droplet Evaporation on a Superhydrophobic Surface. *Langmuir* **2005**, *21*, 11053−11060.
(8) Reyssat, M.; Yeomans, J. M.; Quere, D. Impalement of Fakir Drops. *Europhys. Lett.* **2008**, *81*, 26006.
(9) Reyssat, M.; Pepin, A.; Marty, F.; Chen, Y.; Quere, D. Bouncing Transitions on Microtextured Materials. *Europhys. Lett.* **2006**, *74*, 306−312.
(10) Bartolo, D.; Bouamrirene, F.; Verneuil, E.; Buguin, A.; Silberzan, P.; Moulinet, S. Bouncing or Sticky Droplets: Impalement Transitions on Superhydrophobic Micropatterned Surfaces. *Europhys. Lett.* **2006**, *74*, 299−305.
(11) Bormashenko, E.; Pogreb, R.; Whyman, G.; Bormashenko, Y.; Erlich, M. Vibration-Induced Cassie-Wenzel Wetting Transition on Rough Surfaces. *Appl. Phys. Lett.* **2007**, *90*, 201917.
(12) Kwon, H. M.; Paxson, A. T.; Varanasi, K. K.; Patankar, N. A. Rapid Deceleration-Driven Wetting Transition during Pendant Drop Deposition on Superhydrophobic Surfaces. *Phys. Rev. Lett.* **2011**, *106*, 036102.
(13) Narhe, R. D.; Beysens, D. A. Nucleation and Growth on a Superhydrohobic Grooved Surface. *Phys. Rev. Lett.* **2004**, *93*, 076103.
(14) Wier, K. A.; McCarthy, T. J. Condensation on Ultrahydrophobic Surfaces and Its Effect on Droplet Mobility: Ultrahydrophobic Surfaces Are Not Always Water Repellant. *Langmuir* **2006**, *22*, 2433−2436.
(15) Cheng, Y. T.; Rodak, D. E. Is the Lotus Leaf Superhydrophobic? *Appl. Phys. Lett.* **2005**, *86*, 144101.
(16) Boreyko, J. B.; Chen, C. H. Restoring Superhydrophobicity of Lotus Leaves with Vibration-Induced Dewetting. *Phys. Rev. Lett.* **2009**, *103*, 174502.
(17) Miljkovic, N.; Enright, R.; Wang, E. N. Effect of Droplet Morphology on Growth Dynamics and Heat Transfer during Condensation on Superhydrophobic Nanostructured Surfaces. *ACS Nano* **2012**, *6*, 1776−1785.
(18) Rykaczewski, K. Microdroplet Growth Mechanism during Water Condensation on Superhydrophobic Surfaces. *Langmuir* **2012**, *28*, 7720−7729.
(19) Patankar, N. A. Mimicking the Lotus Effect: Influence of Double Roughness Structures and Slender Pillars. *Langmuir* **2004**, *20*, 8209−8213.
(20) Chen, C. H.; Cai, Q.; Tsai, C.; Chen, C. L.; Xiong, G.; Yu, Y.; Ren, Z. Dropwise Condensation on Superhydrophobic Surfaces with Two-Tier Roughness. *Appl. Phys. Lett.* **2007**, *90*, 173108.
(21) Koch, K.; Bhushan, B.; Jung, Y. C.; Barthlott, W. Fabrication of Artificial Lotus Leaves and Significance of Hierarchical Structure for Superhydrophobicity and Low Adhesion. *Soft Matter* **2009**, *5*, 1386−1393.
(22) Su, Y.; Ji, B.; Zhang, K.; Gao, H.; Huang, Y.; Hwang, K. Nano to Micro Structural Hierarchy Is Crucial for Stable Superhydrophobic and Water-Repellent Surfaces. *Langmuir* **2010**, *26*, 4984−4989.
(23) Cha, T. G.; Yi, J. W.; Moon, M. W.; Lee, K. R.; Kim, H. Y. Nanoscale Patterning of Microtextured Surfaces to Control Superhydrophobic Robustness. *Langmuir* **2010**, *26*, 8319−8326.
(24) Herbertson, D. L.; Evans, C. R.; Shirtcliffe, N. J.; McHale, G.; Newton, M. I. Electrowetting on Superhydrophobic SU-8 Patterned Surfaces. *Sens. Actuators, A* **2006**, *130*, 189−193.
(25) Bahadur, V.; Garimella, S. V. Electrowetting-Based Control of Droplet Transition and Morphology on Artificially Microstructured Surfaces. *Langmuir* **2008**, *24*, 8338−8345.
(26) Krupenkin, T. N.; Taylor, J. A.; Wang, E. N.; Kolodner, P.; Hodes, M.; Salamon, T. R. Reversible Wetting-Dewetting Transitions on Electrically Tunable Superhydrophobic Nanostructured Surfaces. *Langmuir* **2007**, *23*, 9128−9133.

(27) Liu, G.; Fu, L.; Rode, A. V.; Craig, V. S. J. Water Droplet Motion Control on Superhydrophobic Surfaces: Exploiting the Wenzel-to-Cassie Transition. *Langmuir* **2011**, *27*, 2595−2600.
(28) Boreyko, J. B.; Baker, C. H.; Poley, C. R.; Chen, C. H. Wetting and Dewetting Transitions on Hierarchical Superhydrophobic Surfaces. *Langmuir* **2011**, *27*, 7502−7509.
(29) Verho, T.; Korhonen, J. T.; Sainiemi, L.; Jokinen, V.; Bower, C.; Franze, K.; Franssila, S.; Andrew, P.; Ikkala, O.; Ras, R. H. A. Reversible Switching between Superhydrophobic States on a Hierarchically Structured Surface. *Proc. Natl. Acad. Sci. U.S.A.* **2012**, *109*, 10210−10213.
(30) Lee, C.; Kim, C. J. Underwater Restoration and Retention of Gases on Superhydrophobic Surfaces for Drag Reduction. *Phys. Rev. Lett.* **2011**, *106*, 014502.
(31) Lee, C.; Kim, C. J. Wetting and Active Dewetting Processes of Hierarchically Constructed Superhydrophobic Surfaces Fully Immersed in Water. *J. Microelectromech. Syst.* **2012**, *21*, 712−720.
(32) Cheng, Z.; Lai, H.; Zhang, N.; Sun, K.; Jiang, L. Magnetically Induced Reversible Transition between Cassie and Wenzel States of Superparamagnetic Microdroplets on Highly Hydrophobic Silicon Surface. *J. Phys. Chem. C* **2012**, *116*, 18796−18802.
(33) Nosonovsky, M.; Bhushan, B. Patterned Nonadhesive Surfaces: Superhydrophobicity and Wetting Regime Transitions. *Langmuir* **2008**, *24*, 1525−1533.
(34) Kumari, N.; Garimella, S. V. Electrowetting-Induced Dewetting Transitions on Superhydrophobic Surfaces. *Langmuir* **2011**, *27*, 10342−10346.
(35) Quere, D.; Lafuma, A.; Bico, J. Slippery and Sticky Microtextured Solids. *Nanotechnology* **2003**, *14*, 1109−1112.
(36) Enright, R.; Miljkovic, N.; Al-Obeidi, A.; Thompson, C. V.; Wang, E. N. Condensation on Superhydrophobic Surfaces: The Role of Local Energy Barriers and Structure Length Scale. *Langmuir* **2012**, *28*, 14424−14432.
(37) Yu, Y.; Zhao, Z. H.; Zheng, Q. S. Mechanical and Superhydrophobic Stabilities of Two-Scale Surfacial Structure of Lotus Leaves. *Langmuir* **2007**, *23*, 8212−8216.
(38) Noblin, X.; Buguin, A.; Brochard-Wyart, F. Vibrated Sessile Drops: Transition between Pinned and Mobile Contact Line Oscillations. *Eur. Phys. J. E* **2004**, *14*, 395−404.
(39) Brakke, K. A. The Surface Evolver. *Exp. Math.* **1992**, *1*, 141−165.
(40) Hong, S. J.; Chou, T. H.; Chan, S. H.; Sheng, Y. J.; Tsao, H. K. Droplet Compression and Relaxation by a Superhydrophobic Surface: Contact Angle Hysteresis. *Langmuir* **2012**, *28*, 5606−5613.
(41) Hong, S. J.; Chang, C. C.; Chou, T. H.; Sheng, Y. J.; Tsao, H. K. A Drop Pinned by a Designed Patch on a Tilted Superhydrophobic Surface: Mimicking Desert Beetle. *J. Phys. Chem. C* **2012**, *116*, 26487−26495.
(42) Eggers, J.; Dupont, T. F. Drop Formation in a One-Dimensional Approximation of the Navier−Stokes Equation. *J. Fluid Mech.* **1994**, *262*, 205−221.
(43) Shi, X. D.; Brenner, M. P.; Nagel, S. R. A Cascade of Structure in a Drop Falling from a Faucet. *Science* **1994**, *265*, 219−222.
(44) Wilkes, E. D.; Phillips, S. D.; Basaran, O. A. Computational and Experimental Analysis of Dynamics of Drop Formation. *Phys. Fluids* **1999**, *11*, 3577−3598.
(45) Heng, L.; Meng, X.; Wang, B.; Jiang, L. Bioinspired Design of Honeycomb Structure Interfaces with Controllable Water Adhesion. *Langmuir* **2013**, *29*, 9491−9498.
(46) Reyssat, M.; Quere, D. Contact Angle Hysteresis Generated by Strong Dilute Defects. *J. Phys. Chem. B* **2009**, *113*, 3906−3909.
(47) Xu, W.; Choi, C. H. From Sticky to Slippery Droplets: Dynamics of Contact Line Depinning on Superhydrophobic Surfaces. *Phys. Rev. Lett.* **2012**, *109*, 024504.
(48) Raj, R.; Enright, R.; Zhu, Y.; Adera, S.; Wang, E. N. Unified Model for Contact Angle Hysteresis on Heterogeneous and Superhydrophobic Surfaces. *Langmuir* **2012**, *28*, 15777−15788.
(49) Gauthier, A.; Rivetti, M.; Teisseire, J.; Barthel, E. Role of Kinks in the Dynamics of Contact Lines Receding on Superhydrophobic Surfaces. *Phys. Rev. Lett.* **2013**, *110*, 046101.
(50) Yeh, K. Y.; Chen, L. J. Contact Angle Hysteresis on Regular Pillar-Like Hydrophobic Surfaces. *Langmuir* **2008**, *24*, 245−251.
(51) Rykaczewski, K.; Scott, J. H. J.; Rajauria, S.; Chinn, J.; Chinn, A. M.; Jones, W. Three Dimensional Aspects of Droplet Coalescence during Dropwise Condensation on Superhydrophobic Surfaces. *Soft Matter* **2011**, *7*, 8749−8752.
(52) Boreyko, J. B.; Chen, C. H. Self-Propelled Dropwise Condensate on Superhydrophobic Surfaces. *Phys. Rev. Lett.* **2009**, *103*, 184501.
(53) Boreyko, J. B.; Chen, C. H. Self-Propelled Jumping Drops on Superhydrophobic Surfaces. *Phys. Fluids* **2010**, *22*, 091110.
(54) Dietz, C.; Rykaczewski, K.; Fedorov, A. G.; Joshi, Y. Visualization of Droplet Departure on a Superhydrophobic Surface and Implications to Heat Transfer Enhancement during Dropwise Condensation. *Appl. Phys. Lett.* **2010**, *97*, 033104.